



# Evaluation and Comparison of Electromagnetic and Scattering Parameters Data of Two Microstrip Patch Antennas Operating in ISM Band for Cancer Detection

Rabia Top<sup>1\*</sup>, Seyfettin Sinan Gültekin<sup>2</sup> and Dilek Uzer<sup>2</sup>

<sup>1</sup> Karamanoglu Mehmetbey University, Faculty of Engineering, Department of Electrical and Electronics Engineering, Karaman, Turkey (ORCID: 0000-0002-3306-1163)

<sup>2</sup> Konya Technical University, Faculty of Engineering and Natural Sciences, Department of Electrical and Electronics Engineering, Konya, Turkey (ORCID: 0000-0002-6287-9124 and 0000-0003-3850-3810)

(1<sup>st</sup> International Conference on Computer, Electrical and Electronic Sciences ICCEES 2020 – 8-10 October 2020)

(DOI: 10.31590/ejosat.804330)

**ATIF/REFERENCE:** Top, R., Gultekin, S. S. & Uzer, D. (2020). Evaluation and Comparison of Electromagnetic and Scattering Parameters Data of Two Microstrip Patch Antennas Operating in ISM Band for Cancer Detection. *European Journal of Science and Technology*, (Special Issue), 237-244.

## Abstract

Cancer diseases significantly affect lives of many people for last years. The diagnosis and treatment process is quite difficult and painful. It is especially important to reach the result of pathological tissue samples in which the structure of the cancerous tissue is determined and helps to shape the treatment in a short time. Today, it may take days or even months to obtain these results. In this study, microstrip antenna structures that are frequently used due to many advantages in biomedical applications are studied. Electromagnetic field and scattering parameter data of two antennas operating in the 2.45 GHz and 5.8 GHz operating frequency in ISM (Industrial, Scientific and Medical) band region are analyzed and compared. Pathological sample transformed form of tumor and normal skin tissue is simulated and compared in Ansys' HFSS program. Both the electric field values and the S-parameter values were compared by obtaining the values of both antennas at 2.45 GHz and 5.8 GHz from simulations. When looking at the results obtained, the difference rates in the data obtained from the antenna results radiating in the 2.45 GHz region are higher as a percentage. Thus, it is possible to say that it is more advantageous to use the 2.45 GHz frequency in antenna structures used for this purpose compared to the 5.8 GHz radiation area.

**Keywords:** Cancer Detection, Microstrip Patch Antenna, Electric Field, ISM Band, HFSS.

## Kanser Hastalığı Tespitine Yönelik ISM Bandında Çalışan Mikroşerit Yama Yapılı İki Antenin Elektromanyetik Alan ve Saçılma Parametreleri Verilerinin Değerlendirilmesi ve Kıyaslanması

### Öz

Kanser hastalıkları günümüzde birçok insanın hayatını önemli ölçüde etkilemektedir. Teşhis ve tedavi süreci ise oldukça zor ve ağrılıdır. Özellikle kanserli dokunun yapısının belirlendiği ve tedavinin şekillenmesine yardımcı olan patolojik doku örneklerinin sonucuna kısa sürede ulaşmak önemlidir. Günümüzde bu sonuçlara ulaşmak günler hatta aylar sürebilmektedir. Bu çalışmada biyomedikal uygulamalarda birçok avantajı sebebi ile sıkça kullanılan mikroşerit anten yapıları çalışılmaktadır. ISM band bölgesinde bulunan 2.45 GHz ve 5.8 GHz ışınma bölgelerinde çalışan iki adet antenin elektromanyetik alan ve saçılma parametre verileri incelenmekte ve kıyaslanmaktadır. Tümörlü ve normal deri dokusunun patolojik numune dönüştürülmüş hali Ansys'in HFSS programında simüle edilerek kıyaslanmaktadır. Her iki antenin hem 2.45 GHz'deki hem de 5.8 GHz'deki değerleri simülasyonlardan elde edilerek hem elektrik alan değerleri hem de S-parametre değerleri kıyaslanmıştır. Elde edilen sonuçlara bakıldığında, 2.45 GHz bölgesinde ışınma yapan anten sonuçlarından elde edilen verilerdeki farklılık oranları yüzde olarak daha fazladır. Böylelikle bu amaçla kullanılan anten yapılarında 2.45 GHz ışınma bölgesini kullanmanın 5.8 GHz ışınma bölgesini kullanmaya göre daha avantajlı olduğunu söylemek mümkündür.

**Anahtar Kelimeler:** Kanser Tespiti, Mikroşerit Yama Anten, Elektrik Alan, ISM band, HFSS.

\* Corresponding Author: Karamanoglu Mehmetbey University, Faculty of Engineering, Department of Electrical and Electronics Engineering, Karaman, ORCID: 0000-0002-3306-1163, [rabiatorp@kmu.edu.tr](mailto:rabiatorp@kmu.edu.tr)

## 1. Introduction

Pathology, that is the science of disease, can be defined as the study of diseases by scientific methods. Pathology; examines the causes of diseases, how these diseases affect tissues and organs, and the formal and visual characteristics of diseased tissues and organs. For this reason, pathology has an important place in medical science. Pathology is a branch of science that provides easier understanding of diseases by adding the abnormal appearance of diseased organs to the naked eye or under the microscope to the information learned in anatomy and physiology. The contribution of pathological examination to the diagnosis of the disease and the determination of the appropriate treatment method is quite great in areas where tissue forms and appearance are very helpful in decision making. Today, along with the diagnosis of tumors, pathological examination is necessary and mandatory for the definitive diagnosis of many diseases (Patterson, 2014; Nakhleh, 2006).

Evaluation and reporting of tissues can take pathologists sometimes even hours. In addition, depending on the number of patients, it can sometimes take months to report the results of the tissue pieces taken. In addition to all these, considering the human factor, there is no mechanism to check the accuracy of the reports prepared by pathologists based on daily life and human feelings.

Therefore, with this study, it is aimed to provide an initial study to detect a tumor tissue using antenna structures (Mahmud, Islam, Misran, Kibria, & Samsuzzaman, 2018; Ouerghi et al., 2017; Raihan, Alam Bhuiyan, Hasan, Chowdhury, & Farhin, 2017; Rossmann, Rattay, & Haemmerich, 2012). Antennas are used in various biomedical applications. It is possible to find studies on various medical problems in the literature (Catherwood & McLaughlin, 2018; Hasan, Shanto, Howlader, & Jahan, 2018; Meaney et al., 2012; Nalam, Rani, & Mohan, 2014; Nesusudha & Fairy, 2018; Rahaman & Delwar Hossain, 2019; Susila & Fathima, 2017). However, it has not been encountered to examine pathological data with an approach based on antennas structures.

The adaptation of the antenna structures used for various biomedical solutions to the biomedical field has been proven by the studies carried out until today. Microstrip patch antennas are the most preferred structure among these antenna types (Jha et al., 2018; Ketavath, Gopi, & Rani, 2019; Nesusudha & Fairy, 2018; Paracha et al., 2019; Rezaeieh, Antoniadis, & Abbosh, 2018; Sabban, 2018; Tofighi & Pardeshi, 2017; Yan, Soh, & Vandenbosch, 2018; Yilmaz, Foster, & Hao, 2019). Designing microstrip antenna structures in a variety of shapes and sizes is easy and relatively inexpensive. Microstrip antenna structures have been used due to their advantages such as lightness and easy integration into different patch and slot applications (S Dey, Letters, & 1996, n.d.; Supriyo Dey & Mitra, 1996; Lane, Biondi, JS Pleva - US Patent 5, & 1995, n.d.; letters & 1995, n.d.; Luk, Mak, Chow, letters, & 1998, n.d.; Singh & Tripathi, 2011). In the study, the outputs of normal and cancerous skin tissue in two different frequency regions of the microstrip antenna structure taken from a reference source (Yang & Xiao, 2018) and one of our own antenna structure (Top, 2017) were investigated. 2.45 GHz and 5.8 GHz operating frequencies were chosen because they are in the ISM (Industrial, Scientific and Medical) band ("Sinai, Bilim ve Tibbi Elektronik Cihazların İmali ve Kullanılması Hakkında Yönetmelik," 1985). Cancerous and normal skin tissues were modeled in Ansys HFSS program. The scattering parameter values and electric field values obtained with the antenna structures of the pathological sample models introduced to the program were compared. The comparison of data obtained for both 2.45 GHz and 5.8 GHz frequency values is evaluated.

Section 2 explains material and method. Section 3 and 4 presents the results, evaluation and conclusion parts, respectively.

## 2. Material and Method

### 2.1. Antennas Structures

The designed antenna (Figure 1a) and its return loss graphic (Figure 1b) are showed in Figure 1. FR-4 is used as substrate ( $\epsilon_r=4.4$ ). The height is 1.6 mm. A circle with a diameter of 28.84 mm is drawn on the substrate material having a width of 38.3 mm. On the four-axis of the drawn circle, the circles of equal dimensions that have 16 mm diameter are placed. So, antenna radiates at 2.45 GHz as shown in Figure 1. Figure 1b shows the simulation value in the HFSS program and the radiation data of the antenna measured using the network analyzer. As a result of the simulation, it is possible to say that, the return loss value of the antenna structure is -18 dB. And the return loss value is around -40 dB according to the measurement results. As can be seen from the figure, the antenna gives more clear and better radiation values in the free space measurements. For 5.8 GHz radiation area, antenna dimensions: The circle with a diameter of 19 mm is drawn on the substrate material having a width of 38.3 mm. On the four-axis of the drawn circle, the circles of equal dimensions that have 22 mm diameter are placed. Therefore, antenna radiates at 5.8 GHz (Figure 2).

Reference antenna is taken from (Yang & Xiao, 2018). This antenna radiates at 2.45 GHz. It has two layer. One is substrate and other is superstrate. For the layers, Rogers RO6010 ( $\epsilon_r=10.2$ ) is used with thickness of 0.635 mm. Figure 3a shows the antenna structure and Figure 3b shows the return loss graph of this antenna. While adhering the reference, only  $l_1$  and  $l_g$  are changed from patch and substrate dimensions.  $l_1=11$  mm and  $l_g=11.4$  mm are used. Other dimensions are the same with the reference. For 5.8 GHz,  $l_1=35$  mm and  $l_g=50$  mm are found from simulations. Other dimensions are the same with the reference, again. Antenna radiates at 5.6 GHz about 5.8 GHz. This antenna structure is selected because of operating frequency and being a microstrip patch antenna structure.

Total system occurs two same antenna structures. One is a receiver and other is a transceiver. Two antenna types fed by coaxial probe. Interaction between two antennas is important to obtain better data. The data are scattering parameters and electric field values.

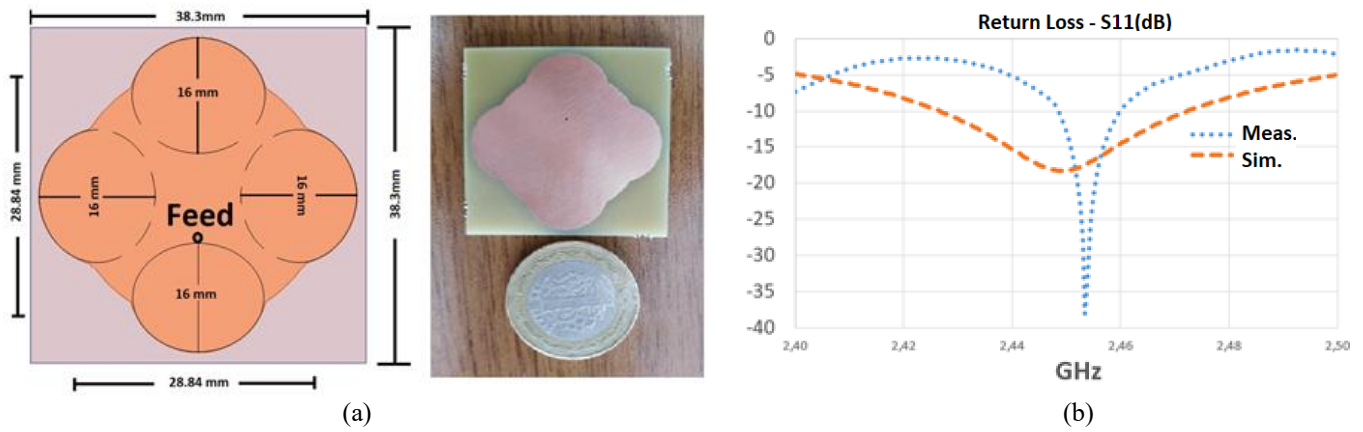


Figure 1. a) antenna structure (top view), b) return loss graph of the proposed antenna.

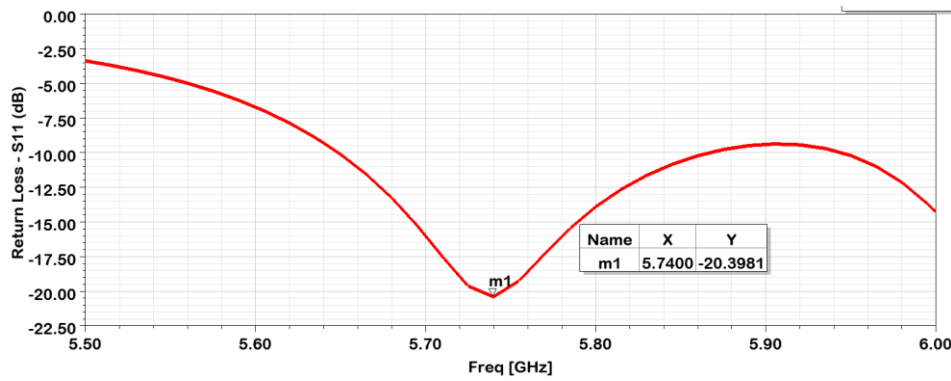


Figure 2. Proposed antenna return loss value at 5.8 GHz

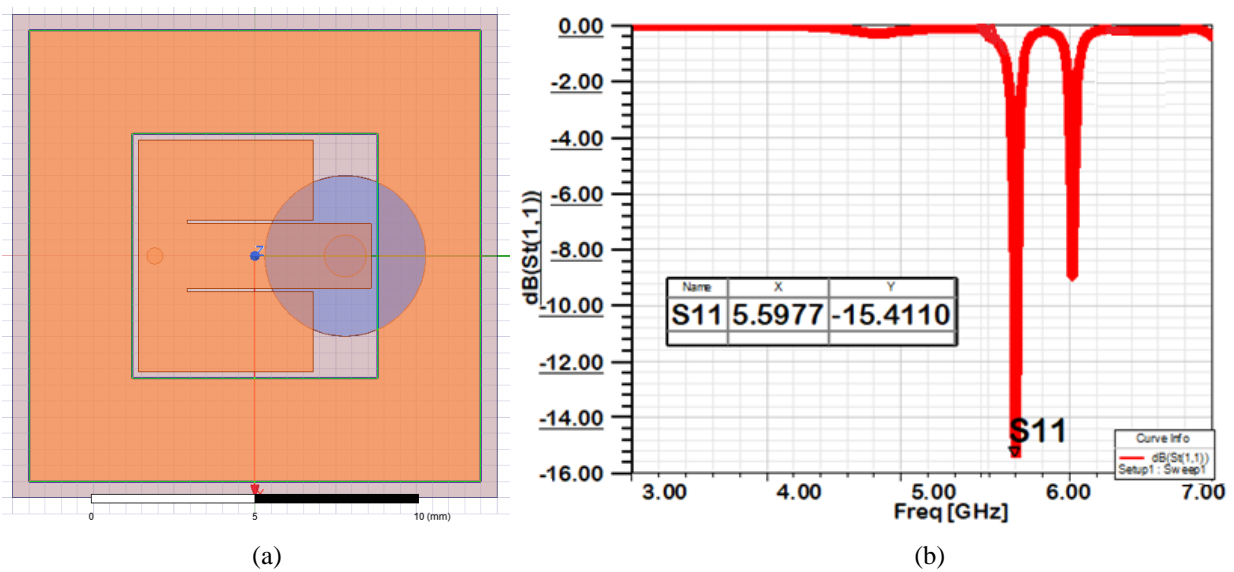


Figure 3. a) antenna structure and b) its return loss value belong to the reference.

## 2.2. Modelled System Structure

Modelled system structure is showed in Figure 4. This system contains a receiver and transeiver antennas, a glass is called “lam”, normal skin tissue and cancerous skin tissue. Biological tissues have different electrical properties like permittivity, permeability and conductivity etc. So, these tissue properties that came from (Gabriel, 1996) are met to HFSS. Normal skin tissue permittivity is 38 and cancerous skin tissue permittivity is 50. “Lam” is a glass, so there is its permittivity in HFSS. Air distance is selected quarter wavelength. Tumor and skin tissue dimensions are about 25 mm such as a “lam”. And tissue thickness is 5 um because of pathological tissue dimensions that is about 3-5 um.

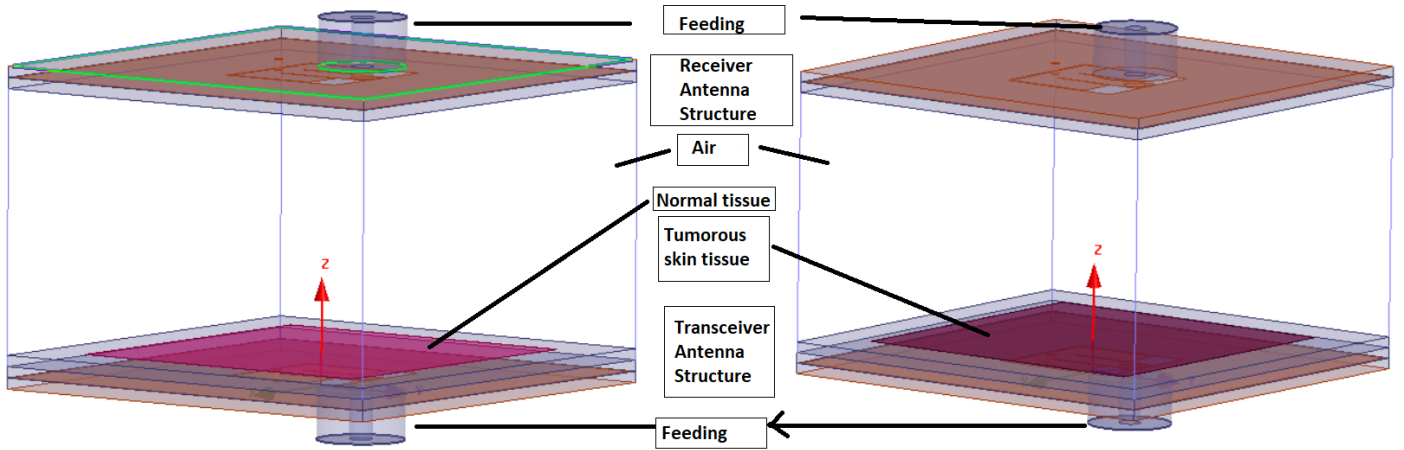


Figure 4. Modelled system structure

### 3. Results and Evaluation

After simulations, electric field and scattering parameter values are obtained. Scattering parameters are also called S-parameters. S-parameters describe the response of an N-port network to signal(s) incident to any or all of the ports (Figure 5). Equation 3.1 explains the parameter values. The first number in the subscript refers to the responding port, while the second number refers to the incident port. Thus  $S_{21}$  means the response at port 2 due to a signal at port 1. The most common "N-port" networks in microwaves are one-port and two-port networks. Here, port number (N) is 2.  $S_{11}$ ,  $S_{21}$ ,  $S_{12}$  and  $S_{22}$  values obtained in dB (Caspers, 2011). These parameters generally explain in dB. While there is S-parameters with tumor and normal skin tissue, values have had from simulation program.

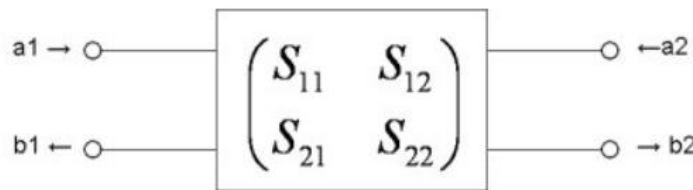


Figure 5. For two port network, S-parameter matrix

$$S_{11} = b_1/a_1, S_{12} = b_1/a_2, S_{21} = b_2/a_1 \text{ and } S_{22} = b_2/a_2 \quad (3.1)$$

Especially in the microwave circuits like this work, electromagnetic field values are important and these values are examined. In the literature, there are a lot of work about electromagnetic field changes of antenna structures. Especially, electric field changes are important, because the biggest difference is of electric field values (Asif, Hansen, Iftikhar, Ewert, & Braaten, 2019; Bao, 2019; Khan, Razzaq, Iqbal, Qamar, & Zubair, 2018; Ma, Sydanheimo, Ukkonen, & Bjorninen, 2018; Nesasudha & Fairy, 2018; Paracha et al., 2019; Rong, Leeson, Higgins, & Lu, 2018; Zamani, Ahdi Rezaeieh, Bialkowski, & Abbosh, 2018).

Table 1 shows the obtained electric field values both proposed and reference antenna structures according to operating frequencies. It can see that the Difference values between normal and tumorous skin tissue. Also, electric field values could be able as a data table from HFSS. These values are in mV because, obtained data table that gives the values as  $rE$ . That is mV because, the electric field value is given by multiplying the angular distance (Canonsburg, 2020). Electric field values are got according to  $\phi$  and  $\theta$  angles. While  $\phi=0^\circ$  and  $90^\circ$ ,  $\theta$  changes from  $0^\circ$  to  $180^\circ$  by  $10^\circ$  step. According to obtained data table values at 5.8 GHz for reference antenna type, evaluations are given below:

- When  $\phi = 0^\circ$ , at  $\theta = 130^\circ$  electric field data, the greatest difference between normal and tumorous tissue is found to be 502.22 mV. This value increases by 11% compared to the arithmetic mean in the case of tumor.
- While  $\phi = 90^\circ$ , the biggest difference in electric field data at  $\theta = 160^\circ$  is found as 501.86 mV. This value increases by 42% compared to the arithmetic mean in the case of tumor.
- The biggest difference between these percentages was found to be 76% at  $\theta = 180^\circ$  while  $\phi = 260^\circ$ , based on the differences between arithmetic means obtained.
- When  $\phi = 40^\circ$ , if  $\theta = 150^\circ$ , the electric field difference between all values obtained is 503.9 mV, which is between tumor and normal tissue.

Since it would be difficult to give each electric field value separately, it is expressed in tabular form. Table 2 and 3 explain the electric field and S-parameter changes while there is tumor in the skin tissue as percent. The arithmetic mean of the values obtained are evaluated as a percentage according to the tumor structure.

Table 1. Obtained electric field graphs for both proposed and reference antenna structure

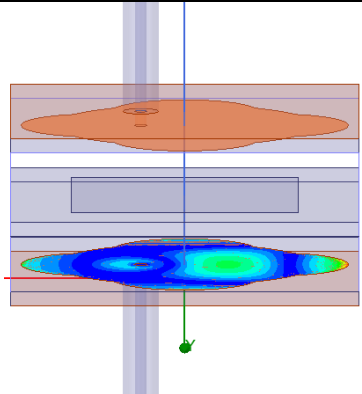
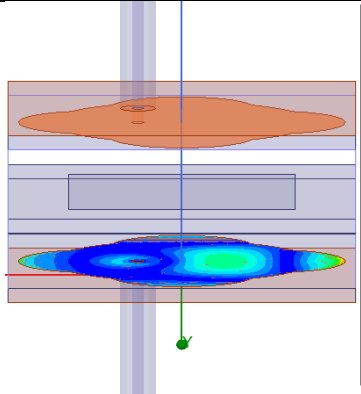
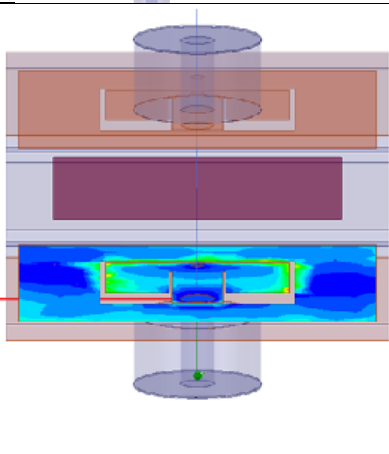
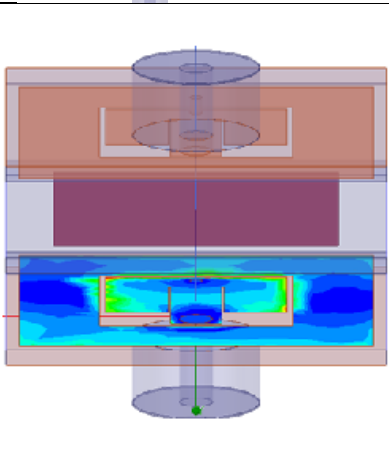
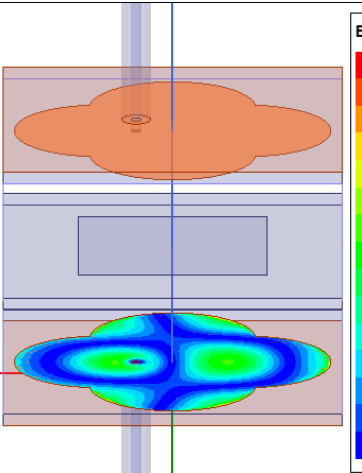
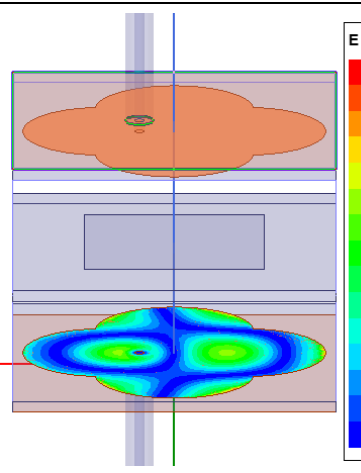
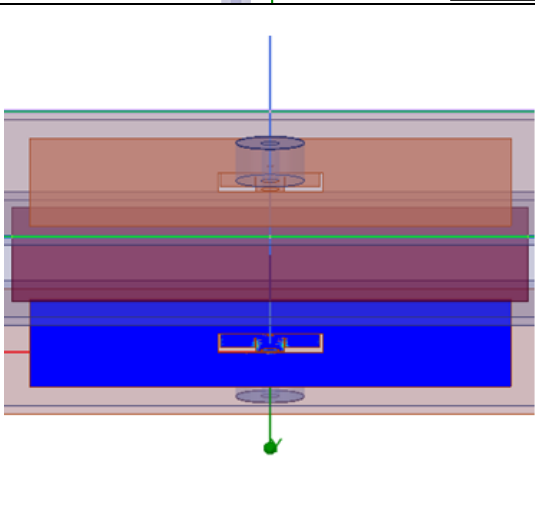
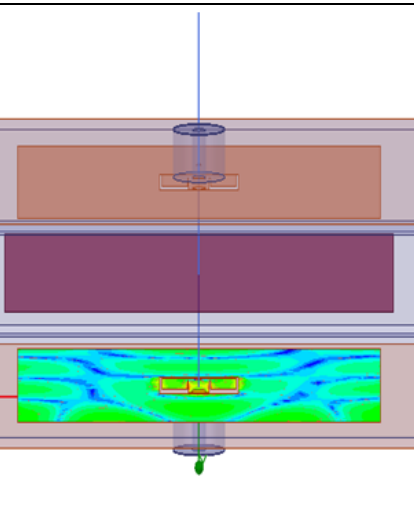
| Frequency type                | Normal skin tissue   | Tumorous skin tissue  |
|-------------------------------|--|---|
| Proposed antenna at 2.45 GHz  |  <p><b>E Field [V/m]</b></p> <ul style="list-style-type: none"> <li>7.6700E+02</li> <li>7.1587E+02</li> <li>6.6474E+02</li> <li>6.1360E+02</li> <li>5.6247E+02</li> <li>5.1133E+02</li> <li>4.6020E+02</li> <li>4.0907E+02</li> <li>3.5793E+02</li> <li>3.0680E+02</li> <li>2.5567E+02</li> <li>2.0453E+02</li> <li>1.5340E+02</li> <li>1.0227E+02</li> <li>5.1133E+01</li> <li>6.7209E-15</li> </ul>   |  <p><b>E Field [V/m]</b></p> <ul style="list-style-type: none"> <li>8.2807E+02</li> <li>7.7286E+02</li> <li>7.1766E+02</li> <li>6.6246E+02</li> <li>6.0725E+02</li> <li>5.5205E+02</li> <li>4.9684E+02</li> <li>4.4164E+02</li> <li>3.8643E+02</li> <li>3.3123E+02</li> <li>2.7602E+02</li> <li>2.2082E+02</li> <li>1.6561E+02</li> <li>1.1041E+02</li> <li>5.5205E+01</li> <li>5.8570E-15</li> </ul>   |
| Reference antenna at 2.45 GHz |  <p><b>E Field [V/m]</b></p> <ul style="list-style-type: none"> <li>5125.4878</li> <li>4783.7886</li> <li>4442.0894</li> <li>4100.3901</li> <li>3758.6912</li> <li>3416.9919</li> <li>3075.2927</li> <li>2733.5935</li> <li>2391.8943</li> <li>2050.1951</li> <li>1708.4960</li> <li>1366.7968</li> <li>1025.0975</li> <li>683.3984</li> <li>341.6992</li> <li>0.0000</li> </ul>                       |  <p><b>E Field [V/m]</b></p> <ul style="list-style-type: none"> <li>4847.6421</li> <li>4524.4985</li> <li>4201.3545</li> <li>3878.2109</li> <li>3555.0669</li> <li>3231.9231</li> <li>2908.7793</li> <li>2585.6355</li> <li>2262.4917</li> <li>1939.3478</li> <li>1616.2039</li> <li>1293.0601</li> <li>969.9163</li> <li>646.7724</li> <li>323.6286</li> <li>0.4848</li> </ul>                        |
| Proposed antenna at 5.8 GHz   |  <p><b>E Field [V/m]</b></p> <ul style="list-style-type: none"> <li>1.2697E+03</li> <li>1.1851E+03</li> <li>1.1005E+03</li> <li>1.0158E+03</li> <li>9.3124E+02</li> <li>8.4664E+02</li> <li>7.6203E+02</li> <li>6.7742E+02</li> <li>5.9282E+02</li> <li>5.0821E+02</li> <li>4.2360E+02</li> <li>3.3900E+02</li> <li>2.5439E+02</li> <li>1.6978E+02</li> <li>8.5177E+01</li> <li>5.7090E-01</li> </ul> |  <p><b>E Field [V/m]</b></p> <ul style="list-style-type: none"> <li>1.1283E+03</li> <li>1.0530E+03</li> <li>9.7784E+02</li> <li>9.0263E+02</li> <li>8.2742E+02</li> <li>7.5221E+02</li> <li>6.7701E+02</li> <li>6.0180E+02</li> <li>5.2659E+02</li> <li>4.5138E+02</li> <li>3.7617E+02</li> <li>3.0096E+02</li> <li>2.2576E+02</li> <li>1.5055E+02</li> <li>7.5340E+01</li> <li>1.3176E-01</li> </ul> |
| Reference antenna at 5.8 GHz  |  <p><b>E Field [V/m]</b></p> <ul style="list-style-type: none"> <li>2.0470E+04</li> <li>1.9105E+04</li> <li>1.7740E+04</li> <li>1.6376E+04</li> <li>1.5011E+04</li> <li>1.3646E+04</li> <li>1.2282E+04</li> <li>1.0917E+04</li> <li>9.5525E+03</li> <li>8.1879E+03</li> <li>6.8232E+03</li> <li>5.4586E+03</li> <li>4.0939E+03</li> <li>2.7293E+03</li> <li>1.3646E+03</li> <li>0.0000E+00</li> </ul> |  <p><b>E Field [V/m]</b></p> <ul style="list-style-type: none"> <li>23543.8359</li> <li>12741.2129</li> <li>6895.1567</li> <li>3731.4487</li> <li>2019.3453</li> <li>1092.8082</li> <li>591.3945</li> <li>320.0447</li> <li>173.1984</li> <li>93.7297</li> <li>50.7237</li> <li>27.4501</li> <li>14.8552</li> <li>8.0392</li> <li>4.3505</li> <li>2.3544</li> </ul>                                   |

Table 2. Electric field changes according to antenna types

| Electric field changes (%) |           |                  |           |                 |           |                  |           |
|----------------------------|-----------|------------------|-----------|-----------------|-----------|------------------|-----------|
| 2.45 GHz                   |           |                  |           | 5.8 GHz         |           |                  |           |
| reference antenna          |           | proposed antenna |           | refence antenna |           | proposed antenna |           |
| Phi=0deg                   | Phi=90deg | Phi=0deg         | Phi=90deg | Phi=0deg        | Phi=90deg | Phi=0deg         | Phi=90deg |
| 11.00                      | 42.00     | -7.60            | -8.07     | -5.20           | -2.62     | 0.03             | 0.54      |

Table 3. S-parameters changes for proposed antenna

| S-parameters changes (%) |      |      |       |         |       |       |       |
|--------------------------|------|------|-------|---------|-------|-------|-------|
| 2.45 GHz                 |      |      |       | 5.8 GHz |       |       |       |
| S11                      | S12  | S21  | S22   | S11     | S12   | S21   | S22   |
| 0.02                     | 0.26 | 0.36 | -0.57 | -0.15   | -0.26 | -0.28 | -0.08 |

Table 2 shows the electric field changes according to antenna type as percent and shows the percentage change in the presence of a tumorous skin tissue. When these values examine and there is tissue with cancerous skin, percentage changes are important for the success of the study. Minus values explain that electric field value is high while there is tumor. So, the values are negative. What matters here is the percentage change.

Table 3 expresses the S-parameter changes for proposed antenna and refers to the percentage comparison of the value obtained in the presence of tumor to normal values. The negative values are because of that S-parameter values are high while there is tumor. For reference antenna structure, obtained S-parameter values are not expressive, so those values are not evaluated.

When the graph values and percentage change values in the tables are examined, the differences between tumor and normal tissue are clearly seen. These differences are quite significant due to the change in the presence of tumor tissue.

#### 4. Conclusions and Recommendations

In the study, two microstrip antennas were evaluated at two different ISM frequencies in order to ensure that pathological sample tissues emerging after long periods of time in the field of pathology were reported in a short time. Pathological result reports are produced by pathologists. It can sometimes take months to print out reports produced based on humanitarian situations. The duration of pathological output reports is very important, especially in cancer patients who are in an emergency or whose treatment needs to be started quickly. Here is an initial study to serve this purpose.

Two biomedical microstrip antenna structures designed and taken as reference were examined. 2.45 GHz and 5.8 GHz ISM band frequencies were used in the study. ISM band is the allowed frequency regions for biomedical solutions. Another reason for choosing these two frequency regions is to be able to compare which of these bands will be more suitable for such a study. It is not difficult to find substrate materials used in the FR-4 and Roger RO6010 in the market to be able to apply them. Antenna structures have been selected that can be useful in design, production and measurement points.

Electric field and scattering parameters are two important expressions in antenna structures. The behavior of the antennas is expressed in scattering parameters. Electromagnetic field values are important due to their microwave radiation. In the study, both electric field and scattering parameter values were examined in order to compare antennas. In order to examine these values and make sense, percentage changes of their arithmetic mean were used. The values obtained were expressed as percentages relative to the tumor structure. The same is true for scattering parameters.

Both angle values are important in electric field values generated according to Theta and Phi angle. Especially when examined in terms of the differences between normal and tumor skin tissue, there are different maximum electric field values. Expressing it as a percentage in the electric field values is important to show the success of the study. Looking at the electric field change table, it is seen that the absolute difference rates at 2.45 GHz are higher. The same is true for scattering parameters. It is seen that choosing the 2.45 GHz operating frequency from both tables can be used to increase the accuracy of the study. In the light of all this information, it is possible to express the suitability of using microstrip antenna structures for a solution to such a system.

Real-time measurements of this system for different microstrip antenna structures and different frequencies will increase the stability of the study.

#### References

Asif, S. M., Hansen, J. W., Iftikhar, A., Ewert, D. L., & Braaten, B. D. (2019). Computation of available RF power inside the body and path loss using in vivo experiments. *IET Microwaves, Antennas and Propagation*, 13(1), 122–126. <https://doi.org/10.1049/iet-map.2018.5582>

- Bao, Z. (2019). Comparative Study of Dual-Polarized and Circularly-Polarized Antennas at 2.45 GHz for Ingestible Capsules. *IEEE Transactions on Antennas and Propagation*, 67(3), 1488–1500. <https://doi.org/10.1109/TAP.2018.2888819>
- Canonsburg, A. D. (2020). *HFSS Help*. (January).
- Caspers, F. (2011). RF engineering basic concepts: S-parameters. *CAS 2010 - CERN Accelerator School: RF for Accelerators, Proceedings*, (June), 67–93.
- Catherwood, P. A., & McLaughlin, J. (2018). *Internet of Things- Enabled Hospital Wards*. (June), 10–18.
- Dey, S, Letters, R. M.-M. and O. T., & 1996, undefined. (n.d.). Compact microstrip patch antenna. *Wiley Online Library*. Retrieved from [https://onlinelibrary.wiley.com/doi/abs/10.1002/\(SICI\)1098-2760\(199609\)13:1%3C12::AID-MOP4%3E3.0.CO;2-Q?casa\\_token=KJKDr8IHH70AAAAA:7a\\_CJXaWYQtXIPvOPBjt4b8XaIyVVSs2IvX4\\_hWYYSurD1AHf0PUrgYcd\\_x\\_bAySAR\\_q0IP\\_wbZvLA](https://onlinelibrary.wiley.com/doi/abs/10.1002/(SICI)1098-2760(199609)13:1%3C12::AID-MOP4%3E3.0.CO;2-Q?casa_token=KJKDr8IHH70AAAAA:7a_CJXaWYQtXIPvOPBjt4b8XaIyVVSs2IvX4_hWYYSurD1AHf0PUrgYcd_x_bAySAR_q0IP_wbZvLA)
- Dey, Supriyo, & Mittra, R. (1996). Compact microstrip patch antenna. *Microwave and Optical Technology Letters*, 13(1), 12–14. [https://doi.org/10.1002/\(sici\)1098-2760\(199609\)13:1<12::aid-mop4>3.0.co;2-q](https://doi.org/10.1002/(sici)1098-2760(199609)13:1<12::aid-mop4>3.0.co;2-q)
- Gabriel, C. (1996). Compilation of the Dielectric Properties of Body Tissues at RF and Microwave Frequencies. *Environmental Health, Report No.* (June), 21. [https://doi.org/Report N.AL/OE-TR- 1996-0037](https://doi.org/Report%20N.AL/OE-TR-1996-0037)
- Hasan, R. R., Shanto, M. A. H., Howlader, S., & Jahan, S. (2018). A novel design and miniaturization of a scalp implantable circular patch antenna at ISM band for biomedical application. *2017 Intelligent Systems Conference, IntelliSys 2017, 2018-Janua*(September), 166–169. <https://doi.org/10.1109/IntelliSys.2017.8324286>
- Jha, A. K., Akhter, Z., Tiwari, N., Muhammed Shafi, K. T., Samant, H., Jaleel Akhtar, M., & Cifra, M. (2018). Broadband Wireless Sensing System for Non-Invasive Testing of Biological Samples. *IEEE Journal on Emerging and Selected Topics in Circuits and Systems*, 8(2), 251–259. <https://doi.org/10.1109/JETCAS.2018.2829205>
- Ketavath, K. N., Gopi, D., & Rani, S. S. (2019). In-vitro test of miniaturized CPW-fed implantable conformal patch antenna at ISM band for biomedical applications. *IEEE Access*, 7, 43547–43554. <https://doi.org/10.1109/ACCESS.2019.2905661>
- Khan, Z., Razaq, A., Iqbal, J., Qamar, A., & Zubair, M. (2018). Double circular ring compact antenna for ultra-wideband applications. *IET Microwaves, Antennas and Propagation*, 12(13), 2094–2097. <https://doi.org/10.1049/iet-map.2018.5245>
- Lane, J., Biondi, J., JS Pleva - US Patent 5, 400,040, & 1995, undefined. (n.d.). Microstrip patch antenna. In *Google Patents*. Retrieved from <https://patents.google.com/patent/US5400040A/en>
- letters, R. W.-E., & 1995, undefined. (n.d.). Small microstrip patch antenna. *Ieeexplore.Ieee.Org*. Retrieved from [https://ieeexplore.ieee.org/abstract/document/383981/?casa\\_token=GusqxrKXU4kAAAAA:DVg-E9gEz7PIX2OxuuUj3W3CEn9Xyk3tPtg-GI5xwt5C9svbJRSJV0wPNaQBo7dX\\_8mWzIv2kgI](https://ieeexplore.ieee.org/abstract/document/383981/?casa_token=GusqxrKXU4kAAAAA:DVg-E9gEz7PIX2OxuuUj3W3CEn9Xyk3tPtg-GI5xwt5C9svbJRSJV0wPNaQBo7dX_8mWzIv2kgI)
- Luk, K., Mak, C., Chow, Y., letters, K. L.-E., & 1998, undefined. (n.d.). Broadband microstrip patch antenna. *Ieeexplore.Ieee.Org*. Retrieved from [https://ieeexplore.ieee.org/abstract/document/706205/?casa\\_token=7knTzGotAAgAAAAA:nxRcP0CMKrv4tQNJtWm1QO8IPdMTiSQMK1gWTWw5Mm76XkegX3\\_8mH6bAfzAGlxFgYxyFRAiv48](https://ieeexplore.ieee.org/abstract/document/706205/?casa_token=7knTzGotAAgAAAAA:nxRcP0CMKrv4tQNJtWm1QO8IPdMTiSQMK1gWTWw5Mm76XkegX3_8mH6bAfzAGlxFgYxyFRAiv48)
- Ma, S., Sydanheimo, L., Ukkonen, L., & Bjorninen, T. (2018). Split-Ring Resonator Antenna System with Cortical Implant and Head-Worn Parts for Effective Far-Field Implant Communications. *IEEE Antennas and Wireless Propagation Letters*, 17(4), 710–713. <https://doi.org/10.1109/LAWP.2018.2812920>
- Mahmud, M. Z., Islam, M. T., Misran, N., Kibria, S., & Samsuzzaman, M. (2018). Microwave imaging for breast tumor detection using uniplanar AMC Based CPW-fed microstrip antenna. *IEEE Access*, 6, 44763–44775. <https://doi.org/10.1109/ACCESS.2018.2859434>
- Meaney, P. M., Zhou, T., Goodwin, D., Golnabi, A., Attardo, E. A., & Paulsen, K. D. (2012). Bone Dielectric Property Variation as a Function of Mineralization at Microwave Frequencies. *International Journal of Biomedical Imaging*, 2012. <https://doi.org/10.1155/2012/649612>
- Nakhleh, R. E. (2006, July 1). What is quality in surgical pathology? *Journal of Clinical Pathology*, Vol. 59, pp. 669–672. <https://doi.org/10.1136/jcp.2005.031385>
- Nalam, M., Rani, N., & Mohan, A. (2014). Biomedical Application of Microstrip Patch Antenna. *International Journal of Innovative Science and Modern Engineering (IJISME)*, 2(6), 6–8.
- Nesasudha, M., & Fairy, J. J. (2018). Low profile antenna design for biomedical applications. *Proceedings of IEEE International Conference on Signal Processing and Communication, ICSPC 2017, 2018-Janua*(July), 139–142. <https://doi.org/10.1109/CSPC.2017.8305825>
- Ouerghi, K., Fadlallah, N., Smida, A., Ghayoula, R., Fattahi, J., & Boulejfen, N. (2017). Circular antenna array design for breast cancer detection. *2017 Sensors Networks Smart and Emerging Technologies, SENSET 2017, 2017-Janua*(1), 1–4. <https://doi.org/10.1109/SENSET.2017.8125016>
- Paracha, K. N., Rahim, S. K. A., Soh, P. J., Kamarudin, M. R., Tan, K. G., Lo, Y. C., & Islam, M. T. (2019). A Low Profile, Dual-band, Dual Polarized Antenna for Indoor/Outdoor Wearable Application. *IEEE Access*, 7, 33277–33288. <https://doi.org/10.1109/ACCESS.2019.2894330>
- Patterson, J. (2014). *Weedon's Skin Pathology E-Book* (Fourth). Retrieved from [https://www.google.com/books?hl=tr&lr=&id=Y-LTBQAAQBAJ&oi=fnd&pg=PP1&dq=patterson+2014+pathology&ots=U3wha\\_QPa1&sig=0fYB8PC-f3bX5-UQ0robmQaUhFY](https://www.google.com/books?hl=tr&lr=&id=Y-LTBQAAQBAJ&oi=fnd&pg=PP1&dq=patterson+2014+pathology&ots=U3wha_QPa1&sig=0fYB8PC-f3bX5-UQ0robmQaUhFY)
- Rahaman, M. A., & Delwar Hossain, Q. (2019). Design and overall performance analysis of an open end slot feed miniature microstrip antenna for on-body biomedical applications. *1st International Conference on Robotics, Electrical and Signal Processing Techniques, ICREST 2019*, 200–204. <https://doi.org/10.1109/ICREST.2019.8644334>
- Raihan, R., Alam Bhuiyan, M. S., Hasan, R. R., Chowdhury, T., & Farhin, R. (2017). Aearable microstrip patch antenna for detecting brain cancer. *2017 IEEE 2nd International Conference on Signal and Image Processing, ICSIP 2017, 2017-January*, 432–436.

- <https://doi.org/10.1109/SIPROCESS.2017.8124578>
- Rezaeieh, S. A., Antoniadis, M. A., & Abbosh, A. M. (2018). Compact and unidirectional resonance-based reflector antenna for wideband electromagnetic imaging. *IEEE Transactions on Antennas and Propagation*, 66(11), 5773–5782. <https://doi.org/10.1109/TAP.2018.2866516>
- Rong, Z., Leeson, M. S., Higgins, M. D., & Lu, Y. (2018). Nano-rectenna powered body-centric nano-networks in the terahertz band. *Healthcare Technology Letters*, 5(4), 113–117. <https://doi.org/10.1049/htl.2017.0034>
- Rossmann, C., Rattay, F., & Haemmerich, D. (2012). Platform for patient-specific finite-element modeling and application for radiofrequency ablation. *Visualization, Image Processing and Computation in Biomedicine*, 1(1). <https://doi.org/10.1615/visualizimageproccomputatbiomed.2012004898>
- Sabban, A. (2018). Small wearable antennas for wireless communication and medical systems. *IEEE Radio and Wireless Symposium, RWS, 2018-Janua*, 161–164. <https://doi.org/10.1109/RWS.2018.8304974>
- SINAİ, BİLİMSEL VE TIBBİ ELEKTRONİK CİHAZLARIN İMALİ VE KULLANILMASI HAKKINDA YÖNETMELİK. (1985, March 22). Retrieved September 19, 2020, from Official Newspaper of Turkish Republic website: <https://mevzuat.kararara.com/mvzt/mvzt3/mvzt1433.html>
- Singh, I., & Tripathi, V. S. (2011). Micro strip Patch Antenna and its Applications: a Survey. In *Article in International Journal of Computer Applications in Technology*. Retrieved from <https://www.researchgate.net/publication/232318276>
- Susila, J. J., & Fathima, H. R. (2017). A Slot Loaded Rectangular Microstrip Patch Antenna for Breast Cancer Detection. *International Research Journal of Engineering and Technology (IRJET)*, 4(4), 3394–3397. Retrieved from <https://www.irjet.net/archives/V4/i4/IRJET-V4I4811.pdf>
- Tofighi, M. R., & Pardeshi, J. R. (2017). Interference Enhanced Biomedical Antenna for Combined Heating and Radiometry Application. *IEEE Antennas and Wireless Propagation Letters*, 16, 1895–1898. <https://doi.org/10.1109/LAWP.2017.2685503>
- Top, R. (2017). *A transmitter microstrip antenna design and application towards the detection of heart disease parameters*. Selcuk University.
- Yan, S., Soh, P. J., & Vandenbosch, G. A. E. (2018). Wearable ultrawideband technology- A review of ultrawideband antennas, propagation channels, and applications in wireless body area networks. *IEEE Access*, 6, 42177–42185. <https://doi.org/10.1109/ACCESS.2018.2861704>
- Yang, Z. J., & Xiao, S. (2018). A wideband implantable antenna for 2.4 GHz ISM band biomedical application. *2018 IEEE International Workshop on Antenna Technology, IWAT2018 - Proceedings*, 1–3. <https://doi.org/10.1109/IWAT.2018.8379168>
- Yilmaz, T., Foster, R., & Hao, Y. (2019). Radio-frequency and microwave techniques for non-invasive measurement of blood glucose levels. *Diagnostics*, 9(1), 1–34. <https://doi.org/10.3390/diagnostics9010006>
- Zamani, A., Ahdi Rezaeieh, S., Bialkowski, K. S., & Abbosh, A. M. (2018). Boundary Estimation of Imaged Object in Microwave Medical Imaging Using Antenna Resonant Frequency Shift. *IEEE Transactions on Antennas and Propagation*, 66(2), 927–936. <https://doi.org/10.1109/TAP.2017.2780898>